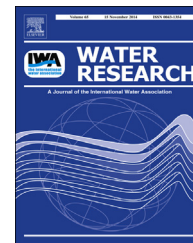




ELSEVIER

Available online at www.sciencedirect.com

ScienceDirect

journal homepage: www.elsevier.com/locate/watres

CrossMark

First report of the successful operation of a side stream supersaturation hypolimnetic oxygenation system in a eutrophic, shallow reservoir

Alexandra B. Gerling^{a,*}, Richard G. Browne^b, Paul A. Gantzer^c,
Mark H. Mobley^d, John C. Little^b, Cayelan C. Carey^a

^a Department of Biological Sciences, Derring Hall, Virginia Tech, Blacksburg, VA 24061, USA

^b Department of Civil and Environmental Engineering, Durham Hall, Virginia Tech, Blacksburg, VA 24061, USA

^c Gantzer Water Resources Engineering, LLC, Kirkland, WA 98034, USA

^d Mobley Engineering Inc., Norris, TN 37828, USA

ARTICLE INFO

Article history:

Received 1 June 2014

Received in revised form

28 August 2014

Accepted 1 September 2014

Available online 10 September 2014

Keywords:

Hypoxia

Internal loading

Iron

Manganese

Phosphorus

Water quality management

ABSTRACT

Controlling hypolimnetic hypoxia is a key goal of water quality management. Hypoxic conditions can trigger the release of reduced metals and nutrients from lake sediments, resulting in taste and odor problems as well as nuisance algal blooms. In deep lakes and reservoirs, hypolimnetic oxygenation has emerged as a viable solution for combating hypoxia. In shallow lakes, however, it is difficult to add oxygen into the hypolimnion efficiently, and a poorly designed hypolimnetic oxygenation system could potentially result in higher turbidity, weakened thermal stratification, and warming of the sediments. As a result, little is known about the viability of hypolimnetic oxygenation in shallow bodies of water. Here, we present the results from recent successful tests of side stream supersaturation (SSS), a type of hypolimnetic oxygenation system, in a shallow reservoir and compare it to previous side stream deployments. We investigated the sensitivity of Falling Creek Reservoir, a shallow ($Z_{\max} = 9.3$ m) drinking water reservoir located in Vinton, Virginia, USA, to SSS operation. We found that the SSS system increased hypolimnetic dissolved oxygen concentrations at a rate of ~ 1 mg/L/week without weakening stratification or warming the sediments. Moreover, the SSS system suppressed the release of reduced iron and manganese, and likely phosphorus, from the sediments. In summary, SSS systems hold great promise for controlling hypolimnetic oxygen conditions in shallow lakes and reservoirs.

© 2014 Elsevier Ltd. All rights reserved.

1. Introduction

Hypolimnetic hypoxia (defined as dissolved oxygen concentrations < 2 mg/L; Wyman and Stevenson, 1991) in lakes and

reservoirs degrades water quality and can prevent recovery from eutrophication (Cooke and Kennedy, 2001; Cooke et al., 2005; Wetzel, 2001). Maintaining an oxygenated environment in the bottom waters prevents the release of nutrients and

* Corresponding author. Tel.: +1 540 231 6679; fax: +1 540 231 9307.

E-mail address: alexg13@vt.edu (A.B. Gerling).

<http://dx.doi.org/10.1016/j.watres.2014.09.002>

0043-1354/© 2014 Elsevier Ltd. All rights reserved.

reduced metals – namely, phosphorus (P), iron (Fe), manganese (Mn) – and their accumulation in the hypolimnion (Matthews and Effler, 2006; McGinnis and Little, 2002; Mortimer, 1941). Controlling these nutrients and metals is essential for improving water quality. Phosphorus can stimulate algal growth and exacerbate eutrophication (Schindler, 1977; Schindler et al., 2008; Smith, 1982), while Fe and Mn in the hypolimnion can cause taste, odor, and color problems for drinking water suppliers (AWWA, 1987; Zaw and Chiswell, 1999). Ultimately, maintaining an oxygenated hypolimnion is paramount for controlling these nutrients and metals and simplifying the water treatment process.

Hypolimnetic oxygenation systems are commonly used to increase dissolved oxygen (DO) concentrations in the hypolimnia of lakes and reservoirs (Beutel and Horne, 1999; Singleton and Little, 2006). Hypolimnetic oxygenation systems aim to maintain thermal stratification while adding oxygen to bottom waters (Beutel and Horne, 1999). Two primary advantages of hypolimnetic oxygenation systems are higher oxygen solubility in comparison to hypolimnetic aeration systems, and higher oxygen transfer efficiencies (percent uptake of delivered oxygen; Beutel and Horne, 1999). As a result, >30 hypolimnetic oxygenation systems have been deployed in lakes and reservoirs around the world, as documented in the literature (Liborius et al., 2009; Noll, 2011; Singleton and Little, 2006; Yajima et al., 2009; Zaccara et al., 2007).

Despite its promise, the process of hypolimnetic oxygenation has three major potential drawbacks – destratification, hypolimnetic warming, and induced sediment oxygen demand – that must be taken into account when designing a system. First, hypolimnetic oxygenation aims to raise the oxygen content of the hypolimnion without destratifying the overlying water column (Ashley, 1985). Such mixing could result in the entrainment of nutrients that were once isolated in the hypolimnion to the epilimnion, resulting in elevated nutrient concentrations in the photic zone and increased nutrient availability. Furthermore, partial destratification increases the hypolimnetic volume over which oxygen must be delivered to maintain desired DO concentrations, leading to inefficiency and added costs. Second, hypolimnetic oxygenation aims to avoid warming of the hypolimnion, which could lead to premature overturn, and poses a potential problem for benthic, cold-water organisms (Beutel and Horne, 1999; Wu et al., 2003). Third, hypolimnetic oxygenation may also stimulate increases in sediment and water column oxygen uptake, thereby accelerating hypolimnetic oxygen depletion and diminishing overall performance of the system (Bryant et al., 2011; Gantzer et al., 2009b). Although somewhat counter-intuitive, hypolimnetic oxygenation systems can increase oxygen demand by stimulating aerobic decomposition and chemical demand (Gantzer et al., 2009b; Lorenzen and Fast, 1977; Moore et al., 1996).

There are several different types of oxygenation systems that are commonly deployed in deep (>10 m) lakes and reservoirs. These primarily include bubble-plume diffusers (linear and circular) and submerged down-flow bubble contact chambers such as the Speece Cone (reviewed by Beutel and Horne, 1999; Singleton and Little, 2006). However, these types of systems are generally only deployed in deep lakes and reservoirs because shallow (<10 m) water bodies lack

sufficient depth to ensure that bubbles of injected oxygen dissolve in the hypolimnion or that thermal stratification is not disrupted by system operation (Beutel, 2006; Cooke et al., 2005). Thus, for implementing hypolimnetic oxygenation in shallow lakes and reservoirs, a technique known as side stream supersaturation (SSS) represents a potential alternative (Beutel and Horne, 1999).

SSS may hold great promise for successful hypolimnetic oxygenation of shallow ecosystems. This technique involves withdrawing hypolimnetic water from the lake, injecting concentrated oxygen gas at high pressure, and returning the oxygenated water to the hypolimnion (Singleton and Little, 2006). Due to the small hypolimnetic volume in shallow water bodies, SSS systems may be more effective than other systems in increasing hypolimnetic DO concentrations because they can add more oxygen with low water flow rate, thereby causing less mixing and maintaining thermal structure.

In a comprehensive review of published studies and other reports, we found that side stream systems have been deployed thus far in at least five lakes or reservoirs and three river or tidal ecosystems worldwide (Table 1). We note the difference in our review between side stream systems that inject oxygen into the hypolimnion of water bodies at saturated concentrations (hereafter, side stream hypolimnetic oxygenation) and SSS systems, which inject oxygen at supersaturated concentrations.

The outcome of the previous side stream and SSS deployments has been mixed. While the earliest known deployment in Ottoville Quarry in 1973 ($Z_{\max} = 18$ m) demonstrated that a side stream system could successfully increase hypolimnetic DO concentrations without destratification of the water column (Fast et al., 1975, 1977), later deployments of side stream systems, one an SSS, in Attica Reservoir (Fast and Lorenzen, 1976; Lorenzen and Fast, 1977), Lake Serraiia (Toffolon et al., 2013), and Lake Thunderbird (OWRB, 2012, 2013), all exhibited premature destratification (Table 1). Consequently, there has been no successful deployment of a side stream or SSS system in a shallow (<10 m) lake or reservoir to date.

Given that most lakes and reservoirs worldwide are small and shallow (Downing et al., 2006; Scheffer, 2004), and that improving water quality is a major goal worldwide (MEA, 2005), we investigated the utility of SSS application in a shallow drinking water reservoir. We had two primary objectives. First, we assessed if the SSS system could successfully overcome induced sediment oxygen demand to increase hypolimnetic DO concentrations without triggering destratification or sediment warming. Second, we evaluated how well the system prevented the release of Fe, Mn, and P from the reservoir sediments.

2. Materials and methods

2.1. Study site

Falling Creek Reservoir (FCR) is a small, eutrophic drinking water reservoir near Vinton in Bedford County, southwestern Virginia, USA (37° 18' 12" N, 79° 50' 14" W). FCR is operated and

Table 1 – Overview of known side stream oxygenation systems, listed chronologically by deployment. The line separates systems deployed in lakes and reservoirs (listed first) from river and tidal ecosystems.

Lake name	Location	Z _{max} (m)	Type of system	Year deployed	Outcome	Reference
Ottoville Quarry	Ottoville, Ohio, USA	18	Side stream pumping	1973	Increased DO and maintained thermal stratification	1, 2
Attica Reservoir	Attica, New York, USA	9.4	Side stream pumping	1973	Increased DO; premature destratification due to increased turbulence	3, 4
Lake Serrai	Trentino, Italy	18	Side stream pumping	2006	Increased DO; water column heating and premature destratification	5
Lake Thunderbird	Norman, Oklahoma, USA	17.7	Supersaturated dissolved oxygen (SDOX) system	2011	Increased DO; sediment heating, water column mixing, premature destratification,oxic water did not penetrate the entire hypolimnion	6, 7
Falling Creek Reservoir	Vinton, Virginia, USA	9.3	Side stream supersaturation	2013	Increased DO and maintained thermal stratification	This study
Canning–Swan River	Western Australia, Australia	Typically <1.5, 3–6 m depressions	Side stream supersaturation	1997	Increased DO and reduced internal nutrient loading	8
Grand Bay (estuarine reach of Mississippi Tidal River)	Mississippi, USA	6	Portable side stream supersaturation	2011 (4 day test period)	Difficulty maintaining elevated DO due to diel tidal fluctuations	9
J.C. Boyle Reservoir (riverine portion)	Klamath County, Oregon, USA	12.8	Portable supersaturated dissolved oxygen (SDOX) system	2011 (5 day test period)	Increased DO; no other parameters are reported	10

1 – Fast et al. (1975), 2 – Fast et al. (1977), 3 – Lorenzen and Fast (1977), 4 – Fast and Lorenzen (1976), 5 – Toffolon et al. (2013), 6 – OWRB (2012), 7 – OWRB (2013), 8 – Sherman et al. (2012), 9 – Gantzer (2011), 10 – CH2M HILL (2013).

maintained by the Western Virginia Water Authority (WVWA) and provides drinking water for residents of Roanoke, VA. FCR is located in an undisturbed, forested watershed and receives water primarily from one inflowing stream. The reservoir has a surface area of $1.19 \times 10^{-1} \text{ km}^2$, maximum depth of 9.3 m, mean depth of 4 m, and a volume of $3.1 \times 10^5 \text{ m}^3$, making it substantially smaller and shallower than other lakes and reservoirs in which hypolimnetic oxygenation has been previously studied. Despite the reservoir's small size, FCR does exhibit stable thermal stratification, typically from May to early October, producing a well-defined and discrete hypolimnion suitable for oxygenation. Mean residence time in the reservoir is 200–300 days. During its recent monitoring history, FCR has exhibited summer cyanobacterial blooms associated with taste and odor problems and long periods of hypolimnetic anoxia linked to internal loading of Fe, Mn, and P.

2.2. Data collection and nutrient analysis

We monitored FCR twice a week during the experimental period from April to September 2013. Water column depth profiles of temperature, DO, conductivity, and turbidity were measured at seven sites on a transect from the reservoir dam

to its upstream tributary (Fig. 1) using an SBE 19plus (Seabird Electronics, Bellevue, WA) high-resolution (4 Hz sampling rate) Conductivity, Temperature, and Depth (CTD) profiler. The response time of the DO probe on the CTD was 1.4 s at 20 °C, allowing data to be collected at ~0.1 m increments from the water's surface to just above the sediments. A YSI (YSI Inc., Yellow Springs, OH) ProDOO meter was substituted for the CTD's dissolved oxygen (DO) profile measurements from 3 July to 15 August and measured DO profiles at the seven sites on 0.5 m increments. Comparison of CTD and YSI profiles on the same sampling days yielded nearly identical measurements of DO (within 0.1 mg/L).

We collected water samples to measure total and soluble Fe, Mn, and P concentrations along a depth profile (at the eight discharge depths of the reservoir: 0.1, 0.8, 1.6, 2.8, 3.8, 5.0, 6.2, and 8.0 m) using a 1.2 L Kemmerer bottle (Wildlife Supply Company, Yulee, FL) at the deep hole as well as in the upstream tributary before it entered the reservoir. Samples for total and soluble analyses at each depth were poured directly from the Kemmerer bottle into plastic bottles that had been acid-washed with 1.2 N hydrochloric acid. Soluble samples were filtered through 0.7 µm Whatman GF/F filters, and total and soluble samples were preserved with 15.9 N nitric acid until analysis. We analyzed the samples for total and soluble

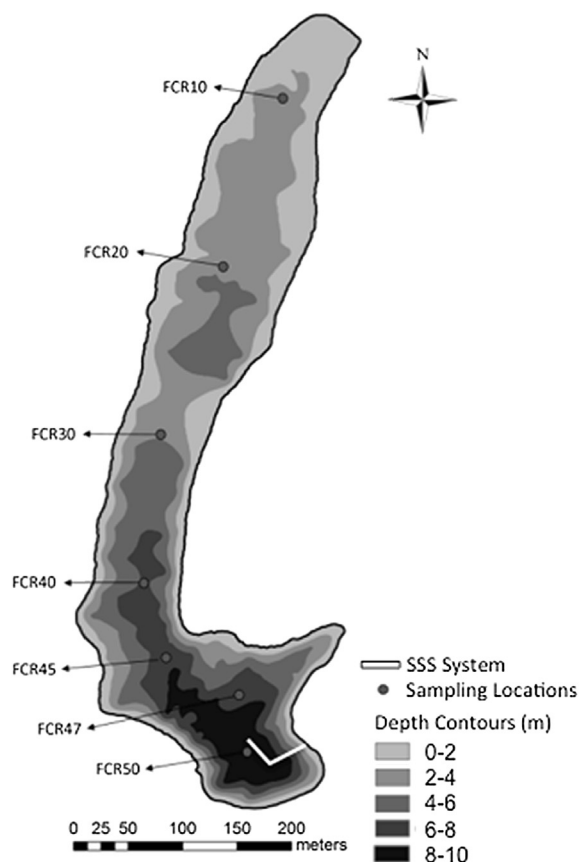


Fig. 1 – Falling Creek Reservoir bathymetry and sample sites, located in Vinton, Virginia, USA. The dots represent sampling locations on a transect from the SSS system to its upstream tributary. The sample locations were labeled based on increasing depths; FCR10 is the shallowest sample location and FCR50 the deepest sample location.

Fe and Mn following the EPA Method 200.8, Rev. 5.4 (1994) using an Agilent 7700x ICP-MS (Agilent Technologies, Santa Clara, CA). We analyzed the samples for total phosphorus (TP) following the EPA Method 365.3 (1978) and soluble reactive phosphate (SRP) on a spectrophotometer following the Quik-Chem Method 10-115-10-1-B.

Finally, we measured the flow rate into the reservoir from the upstream tributary using a rectangular weir with a notch width of 1.10 m. An INW Aquistar PT2X pressure sensor (INW, Kirkland, WA) recorded the water level above the weir every 15 min, which we used to calculate the flow rate of the stream into the reservoir using Chow (1959) and Grant (1991):

$$q = K \times (L - 0.2 \times H) \times H^{1.5} \quad (1)$$

where q is flow rate (m^3/min), K is 110.29, a unit conversion constant, L is the crest length of the weir (m), and H is the head on the weir (m). The residence time of FCR was calculated at 15 min increments using the flow rate of the upstream tributary and assuming the reservoir volume was at full pond, $3.1 \times 10^5 \text{ m}^3$.

2.3. Data analysis

We examined how SSS operation affected hypolimnetic oxygen demand (HOD) and estimated the corresponding induced oxygen demand (IOD) caused by SSS operation. HOD is the rate of change of total oxygen content in the hypolimnion over time, which is measured on both (1) a mass basis (HOD_{mass}) yielding a rate in kg/day, and (2) a concentration basis (HOD_{conc}) yielding a rate in mg/L/day. HOD encompasses all oxygen-consuming processes in the hypolimnion, including oxygen demand from sediment, the water column, and any redox reactions.

We determined HOD and IOD by performing a regression analysis on the volume-weighted oxygen content in the hypolimnion (following the methods of Gantzer et al., 2009b), and then compared HOD and IOD during multiple periods of SSS activation and deactivation. During periods without SSS operation, the rate of change of hypolimnetic oxygen content (HOD_{mass} and HOD_{conc}) was observed to decrease linearly. During SSS operation, the rate of oxygen addition from SSS operation was subtracted from the observed hypolimnetic oxygen accumulation rate, yielding HOD. IOD represents the increased demand above background HOD (calculated only when the SSS was off), which is used to validate the factor of safety employed during system design.

Schmidt stability, an index of the strength of thermal stratification (Idso, 1973), was calculated from the temperature profiles using Lake Analyzer (Read et al., 2011) in Matlab statistical software (version R2013a 8.1.0.604; Mathworks, Natick, MA). Schmidt stability (in J/m^2) indicates the resistance to mechanical mixing due to the potential energy inherent in the stratification of the water column, and was our primary metric for assessing the effect of SSS operation on thermal stratification.

2.3.1. Determining thermocline depth and hypolimnetic oxygen content

We calculated the hypolimnetic volume of the reservoir using the discrete depth temperature data on each sampling day. The thermocline depth was identified by analyzing temperature profiles and identifying the depth that exhibited the maximum rate of change in temperature for each day, following Wetzel (2001). The region of the reservoir below the thermocline depth was identified as the hypolimnion.

We determined hypolimnetic oxygen mass following Gantzer et al. (2009b). As described above, dissolved oxygen profiles were collected at seven sites along the length of the reservoir with a CTD profiler (Fig. 1). We first partitioned the surface area and corresponding volume of the reservoir into seven sections centered around each sampling site. Second, we used the CTD profiles from each sampling site to create a dataset of the DO concentration in 0.1 m thick layers in each reservoir section on every sampling day. Third, we multiplied the oxygen concentration in each 0.1 m layer by the respective volume for that layer to calculate the hypolimnetic oxygen mass. Summing the hypolimnetic layers for each section yielded the total hypolimnetic oxygen mass for that section, and summing all the hypolimnetic sections yielded the oxygen mass for the total hypolimnion. Finally, the summed total hypolimnion oxygen mass was divided by the total hypolimnetic volume to calculate the volume-weighted

hypolimnetic oxygen concentration for the reservoir on each sampling day.

We calculated hypolimnetic oxygen addition and depletion rates using the regression protocol of Lorenzen and Fast (1977), following the methods outlined by Gantzer et al. (2009b). Because hypolimnetic volume was observed to fluctuate between sampling days due to thermocline movement, HOD was calculated both on a mass basis (HOD_{mass}) corrected for volume fluctuations and on a concentration basis (HOD_{conc}) using the volume-weighted hypolimnetic oxygen concentration multiplied by the mean volume for the sampling time period. Both methods yielded similar estimates, within 1%, and thus we report the average of the two calculated HOD estimates here.

2.4. Hypolimnetic oxygen system description and operation

The SSS system was designed and deployed in FCR in September 2012 under the direction of Gantzer Water Resources Engineering, LLC (Kirkland, WA) and Mobley Engineering, Inc. (Norris, TN).

2.4.1. SSS system components

SSS overview: The SSS system installed at FCR consisted of six main components: a submersible pump, inlet piping, oxygen source, oxygen contact chamber, outlet piping, and distribution header (Fig. 2). SSS operation can be summarized as follows. First, hypolimnetic water from a depth of 8.5 m was drawn by a submersible pump into the inlet piping, which transported the water into the oxygen contact chamber. In the oxygen contact chamber, oxygen gas from the oxygen source was injected into the water, resulting in oxygenated water that was supersaturated relative to the oxygen concentrations in the hypolimnion. The oxygenated water exited the oxygen contact chamber through the outlet

piping to the distribution header, which was positioned at the same depth as the submersible piping (8.5 m). The distribution header was where the oxygenated water was injected back into the hypolimnion and was located at the end of the outlet piping. Details for each of the six components are given below.

Submersible pump: Water was withdrawn from the hypolimnion into the inlet piping at a depth of 8.5 m by a Franklin Electric FPS 4400 (10.2 cm) high-capacity submersible pump (Franklin Electric, Fort Wayne, IN) with a corrosion-resistant motor and a delivery capacity of up to 227 liters per minute (LPM). We chose to use a submersible pump for the SSS because a submersible pump, unlike a conventional surface pump, would not lose suction capacity if the reservoir volume was drawn down during drought conditions. A Varispeed P7 pump controller (Yaskawa America, Inc., Waukegan, IL) was used to control and program pump operation. An INW 98i pressure transducer was installed at the highest point of the inlet piping and connected to the pump controller to enable the pump to be pressure-controlled.

Inlet and outlet piping: The inlet and outlet piping systems were each composed of a separate configuration of a three-pipe configuration of a separate supply pipe (inlet or outlet), a ballast pipe, and a buoyancy pipe connected together. The anchoring system consisted of concrete weights connected to the three-pipe configuration with stainless steel cables, and enabled the pipes to be suspended at a fixed depth in the water column (8.5 m depth, or 0.8 m above the reservoir sediments). Of the three pipes in the three-pipe configuration, only the supply pipe was connected into and out of the oxygen contact chamber for the inlet and outlet piping systems, respectively. The supply and ballast pipes were constructed of two 5.1 cm standard-dimension ratio (SDR)-11 high-density polyethylene (HDPE) pipes, and the buoyancy pipe was constructed from 7.6 cm SDR-21 HDPE pipe.

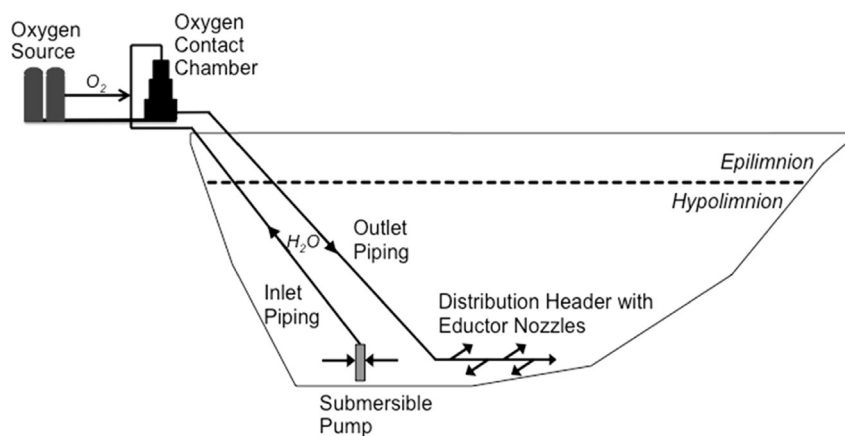


Fig. 2 – A cross-sectional schematic of the SSS system in Falling Creek Reservoir (FCR). The SSS system installed at FCR consisted of six main components: a submersible pump, inlet piping, oxygen source, oxygen contact chamber, outlet piping, and distribution header. As noted in the text, hypolimnetic water from a depth of 8.5 m was drawn by a submersible pump into the inlet piping, which transported the water into the oxygen contact chamber. In the oxygen contact chamber, oxygen gas from the oxygen source was injected into the water, resulting in oxygenated water that was supersaturated relative to the oxygen concentrations in the hypolimnion. The oxygenated water exited the oxygen contact chamber through the outlet piping to the distribution header, which was positioned at the same depth of the submersible piping (8.5 m). The distribution header was located at the end of the outlet piping and was where the oxygenated water was injected back into the hypolimnion.

Traditionally, these piping systems are used for distributing air or oxygen gas to the water column through the supply pipe, and thus the presence of a gas in the supply pipe doubles as ballast. For this system, however, since the mode of oxygen addition was via oxygenated water, an additional pipe filled with gas was needed for ballast. The ballast pipe ensured sufficient flotation to suspend the three-pipe configuration above the reservoir sediments. The larger buoyancy pipe was designed to be able to bring the entire system to the surface, anchors included, for maintenance and was controlled by the volume of water in the pipe. When the water in the buoyancy pipe was ejected, the piping system would rise to the reservoir's surface; it would then be filled with water to sink the system back to the 8.5 m depth in the hypolimnion.

Oxygen source: The oxygen source for the SSS system was a Centrox (AirSep, Buffalo, NY) pressure swing adsorption (PSA) unit. The PSA was capable of delivering enriched oxygen gas (93% nominal purity) up to 15 LPM. The Centrox unit was microprocessor controlled and fed a 227 L volume receiving tank, which was connected to the oxygen contact chamber through an MCP-100SLPM-D-I-485 mass controller (Alicat Scientific, Tucson, AZ).

Oxygen contact chamber: The oxygen contact chamber was constructed from HDPE piping increasing in diameter from 5.1 cm at the top to 30.5 cm at the bottom, with an overall length of 2.7 m.

Distribution header: The distribution header was located at the end of the outlet piping and used evenly spaced 4:1 eductor nozzles (BEX Inc., Ann Arbor, MI) to eject the oxygenated water into the hypolimnion while promoting uniform oxygen distribution. Eductor nozzles were chosen for this application for two reasons: 1) to provide a near-instant dilution of the oxygenated water, which was supersaturated relative to *in situ* conditions, into the hypolimnion; and 2) to promote mixing throughout the hypolimnion via induced flow. For every 1 L of pressurized oxygenated water pumped through an eductor nozzle, 4 L of non-oxygenated water from the hypolimnion were suctioned into the nozzle, resulting in 5 L of volume ejected from the nozzle into the reservoir. Thus, for example, if the pressurized flow from the submersible pump was 10 LPM, the eductor portion of the nozzle suctioned 40 LPM of water from the hypolimnion into the nozzle, and the flow exiting the nozzle was 50 LPM.

We designed the distribution header to cover the length of the deepest region of the reservoir (see Fig. 1) and positioned it to promote uniform mixing throughout the hypolimnion. The distribution header was 76.2 m long with 15 evenly spaced eductor nozzles installed at 4.5 m intervals on alternate sides of the pipe at 8.5 m depth. The nozzles were oriented at a 10° angle above horizontal to minimize re-suspension of sediment. The eductor nozzles were sized to maintain adequate back pressure for optimal oxygen transfer in the contact chamber, while at the same time reducing the exit velocity to avoid sediment re-suspension and thermocline mixing in the hypolimnion.

Ideally, it would be useful to compare the system design and components used in this FCR SSS system with the other side stream systems deployed previously (Table 1). However, we found from our literature review that the engineering designs of those systems were not published or publically

available, or they were lacking sufficient detail to conduct a full comparison.

2.4.2. SSS operational design

The SSS design was based on historical oxygen demand, determined from regression analysis of the volume-weighted HOD during 2008, using the same methods that were applied in 2013 and described above. During the 2008 sampling campaign, we collected DO profiles bi-weekly at the reservoir's deepest site in June and July and observed that the hypolimnion became anoxic on 28 July. We applied a safety factor of five to the background HOD to account for induced demand from SSS operation (Gantzer et al., 2009b) and make-up capacity. Make-up capacity provides an oxygenation system with the ability to recover DO content following an unexpected period of shut down. From the 2008 sampling, we determined that the resulting required oxygen input capacity for summer conditions in FCR was 25 kg/d.

Following the oxygen input requirement determination, we calculated the pumping capacity, minimum velocities for dispersed bubble flow, and system operating pressures needed for successful oxygen transfer into the side stream water flow. We modeled the oxygen contact chamber and corresponding distribution piping with CSFSIM (Compressible Steady Flow SIMulation). CSFSIM modeling was used to determine the duration of time water spent in the distribution pipe, head losses, water velocities, and contact time in the oxygen contact chamber. Henry's law was used to determine the theoretical oxygen concentration for different water flow rates, pressures, and maximum summer temperatures, which follows similar estimates by Ashley (1985) and Ashley et al. (1987).

2.4.3. SSS system startup and testing

During SSS system testing, the oxygen concentration leaving the distribution header was predicted using observed water and applied gas flow rates, and compared to saturation conditions using Henry's law and pressure and temperature values measured with the pressure transducer installed in the inlet piping. Hamilton Oxyferm FDA ARC (Hamilton Company, Reno, NV) oxygen sensors were positioned on the effluent of the oxygen contact chamber and just prior to the first nozzle to validate oxygen transfer capacity and identify system operational limitations. Differences measured between the two readings provided operational guidelines and indicated the overall oxygen transfer efficiency in the oxygen contact chamber.

We activated the SSS system on 14 May 2013 and operated it continuously for five weeks. The system was deactivated on 20 June 2013 and remained off until it was reactivated on 1 August 2013. After the system was reactivated a second time, it remained on for the duration of the experimental monitoring period.

During both activation periods, the SSS was operated to add oxygen to the hypolimnion at 25 kg/d with a pump flow rate set at 227 LPM. At this pump flow rate, the mean hypolimnetic volume during both activation periods (4.4×10^7 L) was actively circulated through the SSS system every 133 days. However, the active circulation induced in the hypolimnion from pump discharge through the eductor nozzles

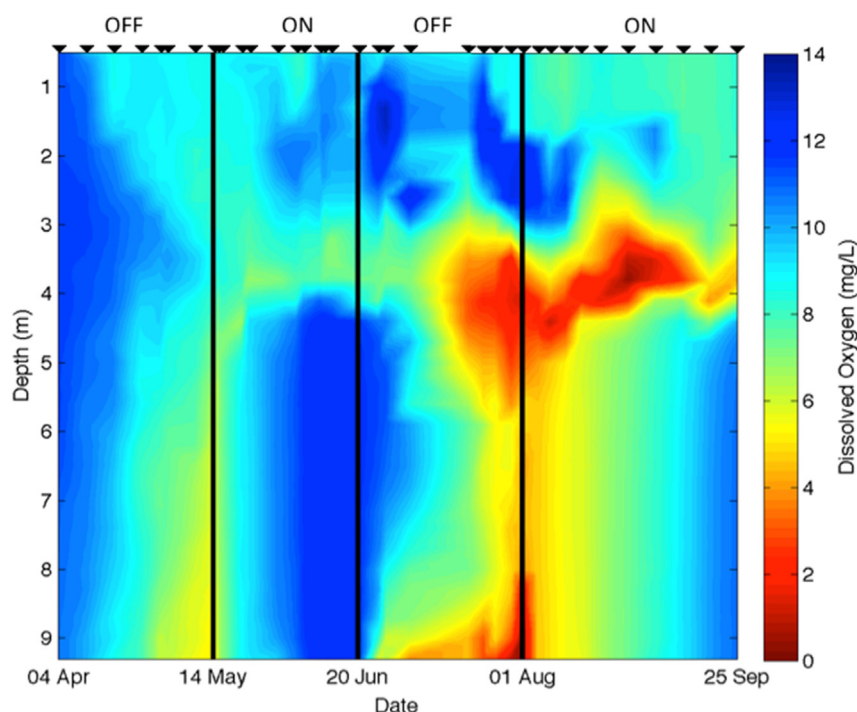


Fig. 3 – Dissolved oxygen concentrations from the deep hole of the reservoir from 4 April to 25 September 2013. The system was deactivated until 14 May (denoted by the “OFF”), activated until 20 June (denoted by the “ON”), deactivated again until 1 August (denoted by the “OFF”), and finally reactivated for the remainder of the sampling period (denoted by the “ON”). All sample days are denoted by inverted black triangles; data were interpolated between sample days for the figure. The distribution header was located at 8.5 m depth.

was estimated to be 1135 LPM, thus mixing the mean hypolimnetic volume every 26 days.

3. Results

3.1. Dissolved oxygen and thermal structure

At the beginning of our sampling period in early April 2013, DO was uniformly distributed throughout an isothermal water column (Fig. 3). As thermal stratification intensified in April and early May, volume-weighted hypolimnetic DO concentrations steadily declined at a mean rate of 0.13 mg/L/d (Fig. 4; we excluded the first three sampling days from this calculation because thermal stratification did not fully develop until 25 April). Prior to SSS activation on 14 May, DO concentrations in the hypolimnion decreased to 5.2 mg/L just above the reservoir sediments.

We observed that SSS activation successfully increased hypolimnetic DO concentrations up to 600 m from the SSS system (Fig. 5) without warming the bottom waters or destratifying the water column (Fig. 6). SSS activation on 14 May resulted in a steady increase in volume-weighted hypolimnetic DO, which linearly increased throughout the operational phase at a mean rate of 0.18 mg/L/d (Fig. 4). Due to the 4:1 eductor nozzles on the distribution header, SSS operation resulted in a well-mixed hypolimnion, with uniform DO concentrations between the thermocline and the sediments.

Oxygen concentrations increased both above and below the distribution header at 8.5 m depth.

Importantly, SSS activation did not decrease thermal stability. On the contrary, Schmidt stability increased throughout the operational phase to its seasonal maximum (48.34 J/m^2) in early July (Fig. 6). This was located at a mean depth of 4.7 m throughout the first operational phase and ranged from 4.4 to 5.0 m. A defined metalimnetic oxygen minimum between ~3 and 4 m depth developed and persisted throughout this operational phase, indicating minimal to no mixing between the hypolimnion and epilimnion.

SSS deactivation on 20 June led to an immediate decrease in DO concentrations (Fig. 3), with the greatest DO depletion occurring near the sediments. During this phase, volume-weighted hypolimnetic DO linearly decreased at a mean rate of 0.18 mg/L/d (Fig. 4), resulting in hypoxic conditions throughout the hypolimnion by 35 days after SSS deactivation. However, DO concentrations at the sediments decreased much more rapidly than in the bulk hypolimnion. Within two weeks after SSS deactivation, the DO concentration had decreased from 11.7 to 3.9 mg/L just above the reservoir sediments, at a rate of 0.57 mg/L/day. Similarly, hypoxia in the metalimnetic region intensified during this period, from 8.8 to 1.4 mg/L. Immediately prior to SSS reactivation on 1 August, DO concentrations were <0.5 mg/L at the sediments. This period also coincided with 7 large (>1 cm/day) rain events, temporarily causing small fluctuations in Schmidt stability (Fig. 6).

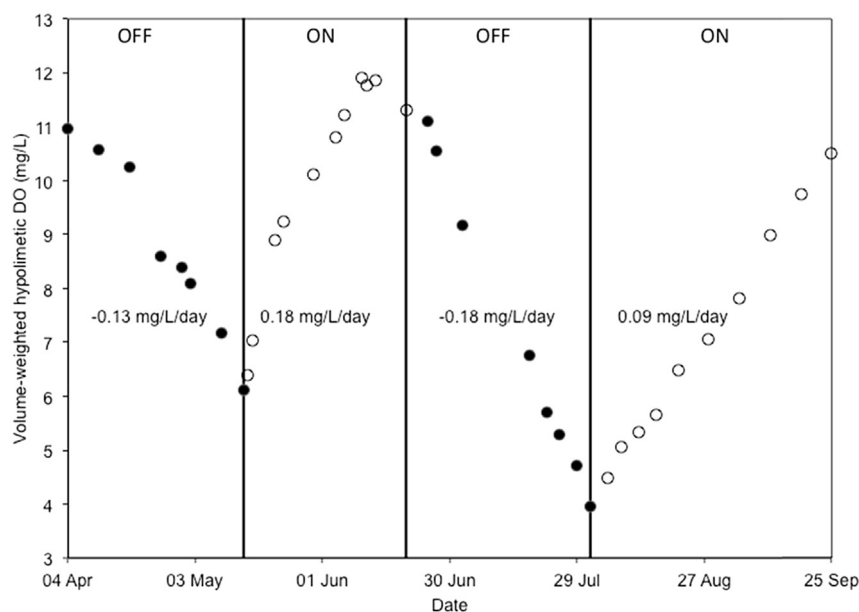


Fig. 4 – Volume-weighted hypolimnetic dissolved oxygen addition and depletion rates in mg/L/day from 4 April to 25 September 2013. The black dots represent when the SSS was deactivated (denoted by the “OFF”), and the white dots represent when the SSS was activated (denoted by the “ON”). The mean depletion and addition rate for each period are embedded in the figure; the first three sampling days were excluded from the first depletion rate calculation because thermal stratification did not fully develop until 25 April.

We reactivated the SSS system on 1 August, which again triggered an immediate increase in DO and restoration of well-mixed conditions in the hypolimnion (Fig. 3). During the second activation phase, volume-weighted hypolimnetic DO linearly increased at the mean rate of 0.09 mg/L/d (Fig. 4). The sediment–water interface exhibited a rapid increase in DO from 0.42 to 4.67 mg/L in the 4 days after activation. Similar to the first operational phase, the thermocline was located at a mean depth of 4.9 m (ranging from 4.6 to 5.6 m) during the second operational phase, with no major visible effects of the SSS on Schmidt stability until thermal stratification naturally weakened in mid-September.

3.2. Hypolimnetic oxygen demand

We observed an increase in hypolimnetic oxygen demand (HOD) during both SSS operational phases compared to the deactivation phases. The HOD in May prior to system activation was 6.5 kg/d, whereas HOD in the first activation phase was 18.6 kg/d, representing an increase of 186%. Similarly, HOD was 6.9 kg/d and 20.7 kg/d during the second deactivation and activation phases, respectively, representing an increase in HOD of 200% when the SSS was activated. During the first operational phase, the induced oxygen demand (IOD), which represents the relative increase in oxygen consumption due to SSS system operation, was estimated to be 2.86, while the IOD in the second operational phase was 3.01.

3.3. Iron, manganese, and phosphorus

Throughout the sampling period, we observed that total and soluble fractions of both Fe and Mn exhibited similar patterns

of nutrient release from the sediments (Fig. 7A–D). Fig. 7 displays concentrations of nutrients and metals during the sampling period. The data are interpolated between sampling days, which are denoted by inverted black triangles, and between sampling depths. The observed hypolimnetic Fe and Mn concentrations throughout the sampling period are displayed in Fig. 8(A–D) without interpolation.

From the beginning of May until the end of July, the concentrations of both fractions of Fe and Mn were below 1 mg/L. On 1 August, after 7 days of hypoxia at the sediment–water interface during SSS deactivation, we observed a large increase in Fe and Mn at the two deeper sampling depths. At 8 m depth, total and soluble Fe concentrations reached maxima of 11.6 mg/L and 2.2 mg/L, respectively, while total and soluble Mn concentrations reached maxima of 4.7 mg/L and 4.7 mg/L, respectively. As shown in Fig. 8, when the SSS was activated on 1 August, Fe and Mn decreased rapidly, and the concentrations of Fe and Mn at the three hypolimnetic sampling depths tended to converge within 1 week after reactivation, indicating mixing of the hypolimnion. During the remainder of the sampling period, total Fe concentrations in the hypolimnion remained between 1.5 and 2 mg/L, while total Mn concentrations remained near 1 mg/L in the hypolimnion. Likewise, soluble Fe and Mn concentrations remained lower than 1 mg/L after 1 August.

In contrast to Fe and Mn, we observed more variable patterns in TP and SRP during the sampling period (Fig. 7E, F). Release of P from the sediments, as indicated by an increase in P concentrations at the bottom of the hypolimnion, was greater overall during SSS deactivation phases than activation phases with peak TP and SRP concentrations of 98.0 $\mu\text{g/L}$ and 9.8 $\mu\text{g/L}$, respectively, at 8 m depth on 25 July (Fig. 8E, F). We also observed elevated P concentrations in the epilimnion during the second SSS deactivation

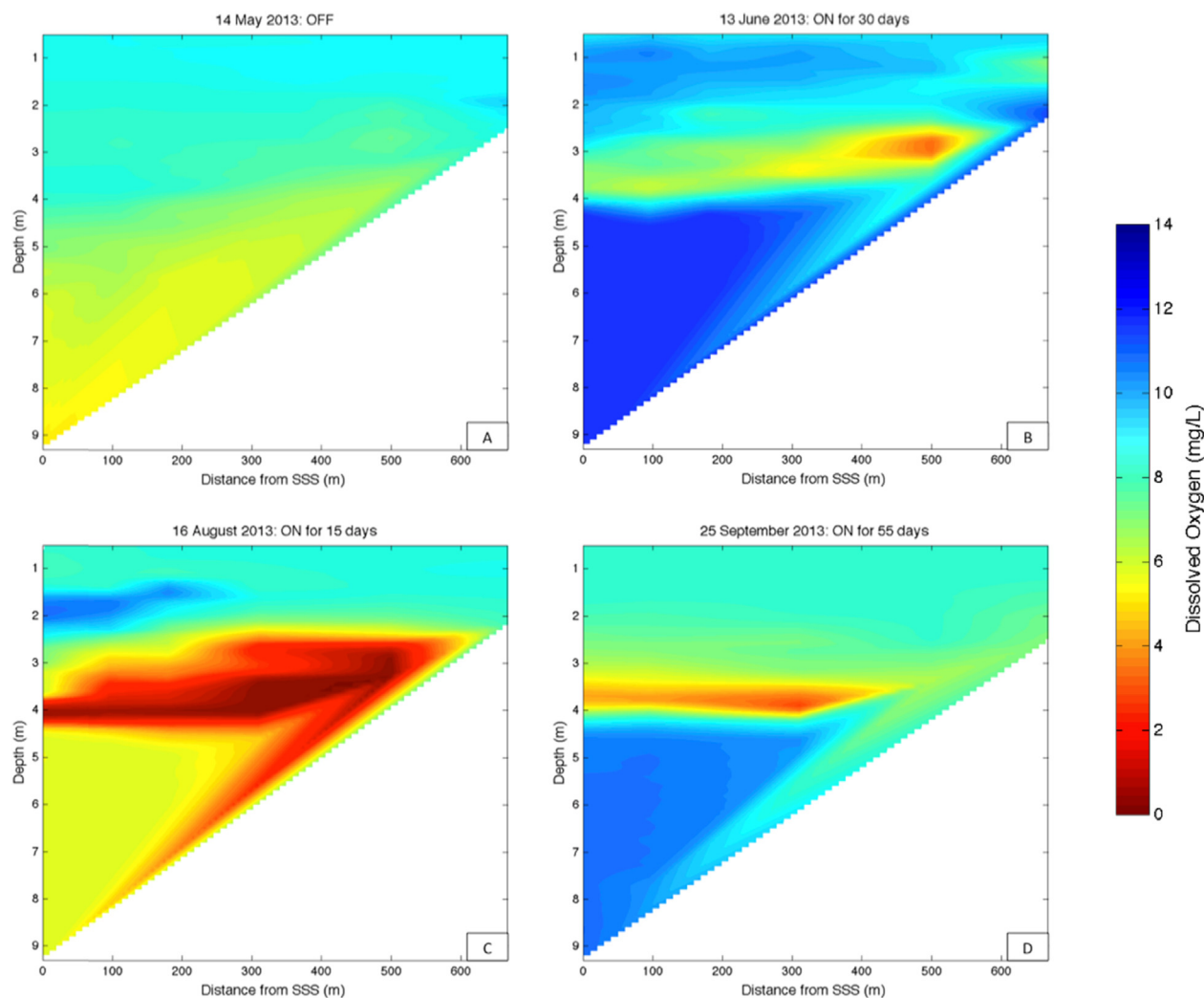


Fig. 5 – Dissolved oxygen concentrations on a transect up the reservoir from the side stream supersaturation (SSS) system to the upstream tributary on four select dates: (A) 14 May 2013, immediately before the SSS was activated for the first time; (B) 13 June, after the SSS was continuously activated for 30 days; (C) 16 August, after the SSS had been deactivated for 42 days and subsequently reactivated for 15 days; and (D) 25 September, after the SSS had been reactivated for 55 days.

tion phase that coincided with the large rain events (Appendix A). TP in the surface waters reached a maximum of 118.8 $\mu\text{g/L}$ and SRP of 22.2 $\mu\text{g/L}$ at 0.8 m on 11 July, a day after the upstream tributary exhibited the maximum flow rate observed during the entire sampling period (21.4 m^3/min) due to a large rain storm (10 cm over the preceding 24 h). Despite this variability in the epilimnion, the total loads of P in the hypolimnion decreased by 50% within 1 week after SSS reactivation, representing a decrease in 1.14 kg of P from the hypolimnion. No increases in any of the measured elements – Fe, Mn, or P – were observed in the hypolimnion during the second oxygenation period.

4. Discussion

4.1. SSS successfully oxygenated the hypolimnion of FCR

Our results indicate that SSS operation was successful in increasing hypolimnetic DO concentrations in FCR, a

eutrophic, shallow reservoir. The two major issues that plagued previous side stream deployments – namely, warming of the hypolimnion and altered thermal stratification (Table 1) – were not observed during the sampling period. Schmidt stability throughout the activation and deactivation phases reflected a pattern typical of seasonal variability, rather than a response to SSS operation. We observed that stratification continued to strengthen during the first SSS operational period, demonstrating that the SSS system was able to successfully oxygenate the hypolimnion uniformly from the sediments to the thermocline without causing the entire water column to mix. The thermal structure was slightly disturbed in July; however, this disturbance coincided with several large rain events and was likely not related to SSS operation.

Furthermore, the consistent strength of the thermocline was likely why a metalimnetic oxygen minimum developed throughout the summer months in FCR. Beginning in July, algae from the epilimnion began to accumulate in the

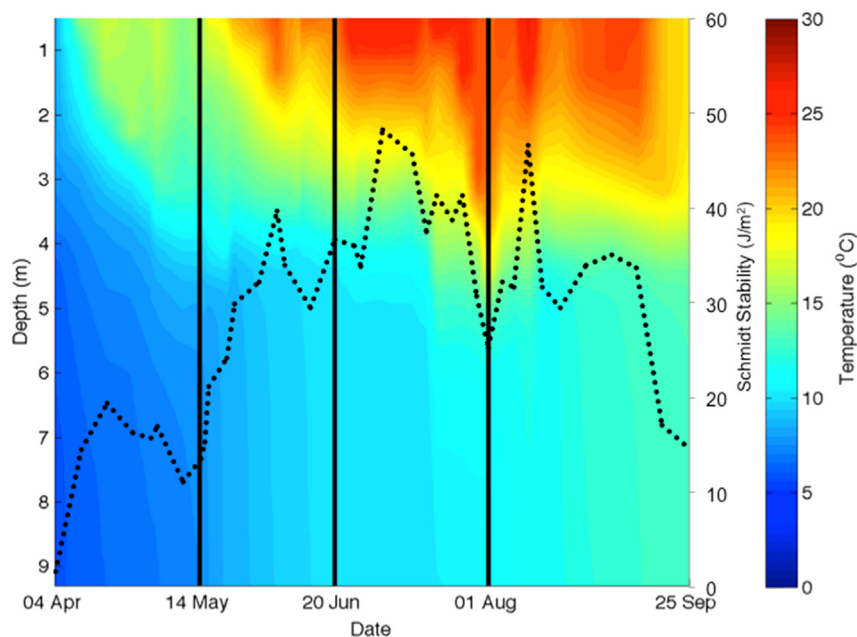


Fig. 6 – Temperature ($^{\circ}\text{C}$, colored heat map) and Schmidt stability values (J/m^2 , dotted line) measured at the deep hole of the reservoir from 4 April to 25 September 2013. The system was deactivated until 14 May (denoted by the “OFF”), activated until 20 June (denoted by the “ON”), deactivated again until 1 August (denoted by the “OFF”), and finally reactivated for the remainder of the sampling period (denoted by the “ON”). The sampling days used to generate the figure were the same as used in Fig. 1.

thermocline and decompose, as evident from the DO data (Fig. 3). This detrital buildup resulted in a disproportionate oxygen demand at this depth, resulting in a metalimnetic oxygen minimum and further demonstrating the strength of the thermocline.

As shown in Table 1, three out of the four previously installed side stream systems resulted in premature destratification. In the three systems that failed, the mixing energy introduced into the hypolimnion was presumably too high, resulting in substantial erosion of the thermocline, warming of the hypolimnion, and subsequent mixing of the destabilized water column. In contrast, the SSS system in FCR added the required amount of oxygen in a relatively low volume of water. One of the advantages of SSS over other hypolimnetic oxygenation systems is that the DO can be raised to higher levels by increasing the pressure in the oxygen contact chamber; i.e., a large amount of oxygen can be added in a small amount of water. Although the DO in the water being delivered to the hypolimnion may be supersaturated at its discharge depth, the discharge jets rapidly dilute the DO, preventing the formation of gas bubbles that are large enough to escape from the hypolimnion. At the same time, energy is needed to spread the oxygenated water throughout the hypolimnion, raising DO to the required concentration. Thus, successful design requires a balance between providing sufficient energy to spread the oxygen, but not so much that thermal stratification in the reservoir is destabilized. As noted above, it would be useful to compare the system design and components used in our SSS system with the other side stream systems deployed previously (Table 1). However, we

found from our literature review that the engineering designs of those systems were not published or publically available, or they were lacking sufficient detail to conduct a full comparison.

Prior to the activation of the SSS in FCR, the side stream system deployed in Ottoville Quarry was the only known system that had successfully increased hypolimnetic DO concentrations while preserving thermal stratification. Ottoville Quarry's maximum depth (18 m) was twice as deep as FCR, thus possessing a larger hypolimnetic volume for oxygenation. Unfortunately, Fe, Mn, and P concentrations were not reported for Ottoville Quarry, so it is unknown if that SSS system was able to suppress internal loading. In addition, little information is available on its SSS engineering design or operation. However, it was reported that the oxygen depletion averaged 1.0 mg/L/week and oxygen addition averaged 0.9 mg/L/week in Ottoville Quarry (Fast et al., 1975), which were coincidentally the same depletion and addition rates observed in FCR. While the system deployed in Ottoville Quarry was based on side stream pumping, not SSS, it provides an important early example of the great potential of side stream hypolimnetic oxygenation in lakes and reservoirs.

4.2. Higher induced oxygen demand during oxygenation

Hypolimnetic oxygen demand encompasses all oxygen-consuming processes in the hypolimnion. In FCR, HOD is likely driven primarily by organic matter decomposition (Davis et al., 1987; Gantzer et al., 2009b). During SSS operation, we observed increased HOD, likely due to higher rates of

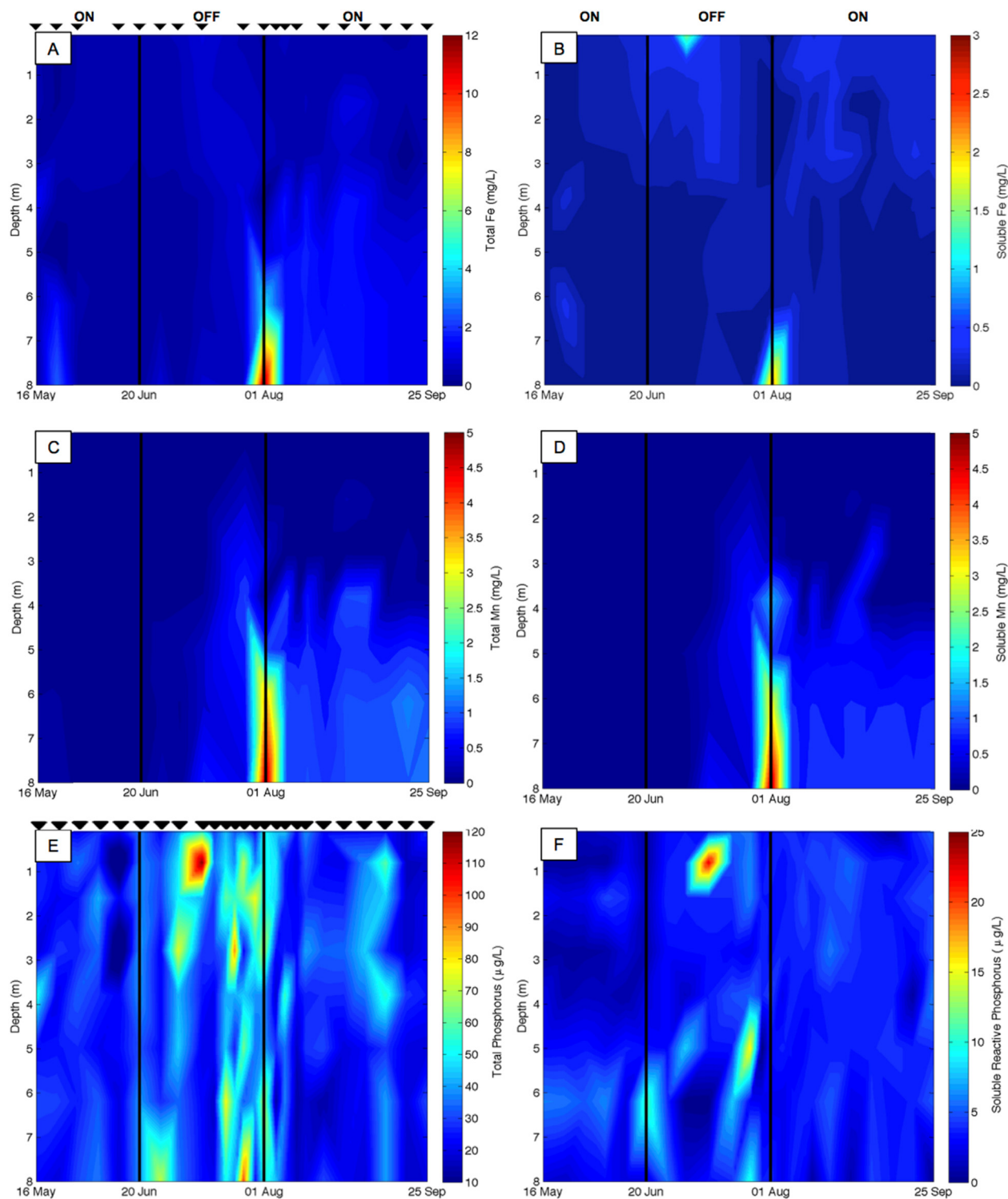


Fig. 7 – The total and soluble fractions of iron (A, B), manganese (C, D), and phosphorus (E, F), respectively. Iron and manganese concentrations are given in mg/L, phosphorus concentrations are given in µg/L. All measurements were sampled at the deepest site of the reservoir from 16 May to 25 September 2013. All sample days are denoted by inverted black triangles; data were interpolated between sample days for the figures. The total and soluble fractions of iron and manganese (panels A–D) had the same sample days, while the total and soluble reactive phosphorus had the same sample days (panels E, F). The system was activated until 20 June (denoted by the “ON”), deactivated again until 1 August (denoted by the “OFF”), and finally reactivated for the remainder of the sampling period (denoted by the “ON”).

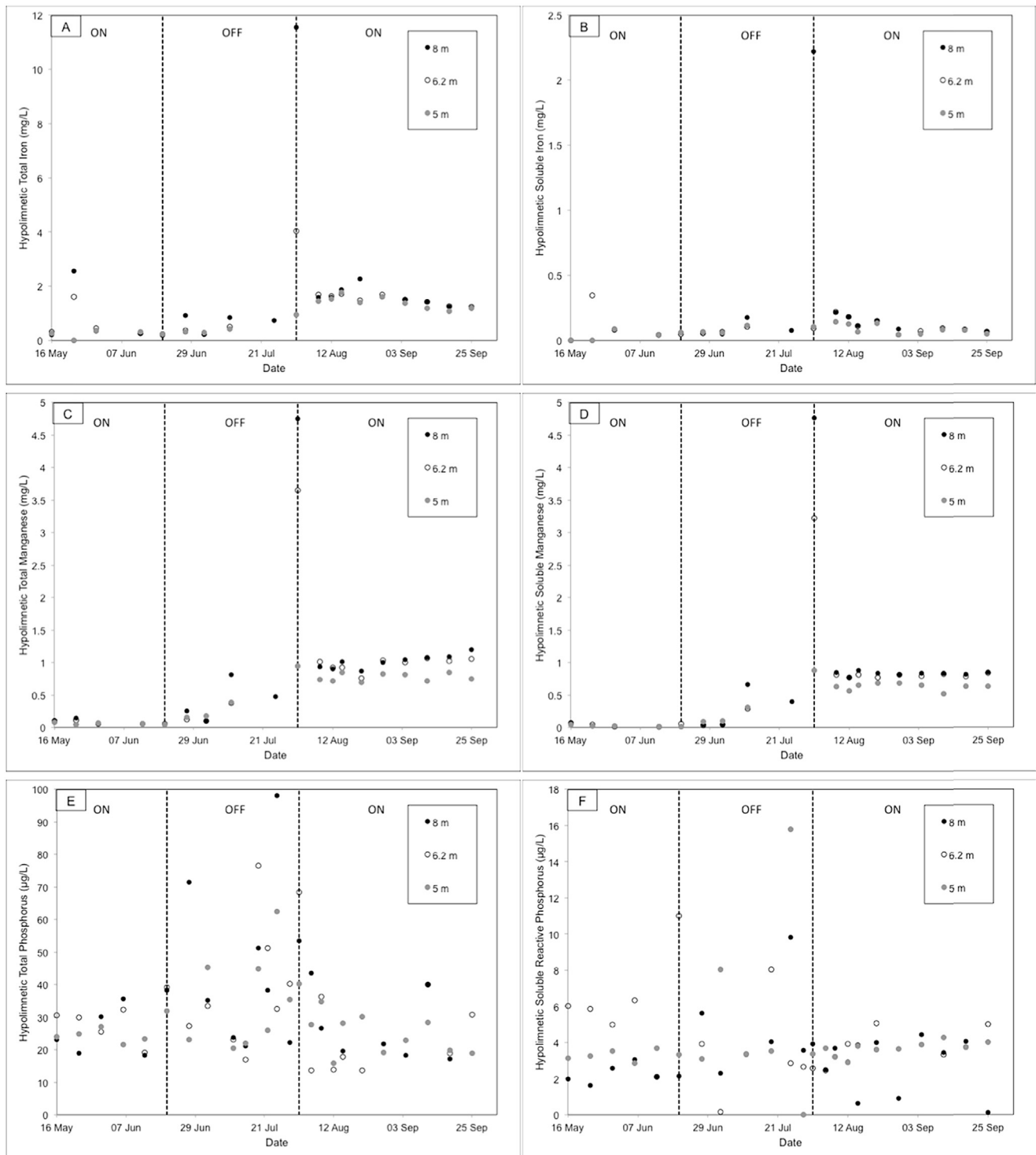


Fig. 8 – The total and soluble fractions of hypolimnetic iron (A, B), manganese (C, D), and phosphorus (E, F), respectively, measured at 5 m, 6.2 m, and 8 m depths in the hypolimnion. Iron and manganese concentrations are given in mg/L, phosphorus concentrations are given in $\mu\text{g/L}$. All measurements were collected at the deepest site of the reservoir from 16 May to 25 September 2013. The system was activated until 20 June (denoted by the “ON”), deactivated again until 1 August (denoted by the “OFF”), and finally reactivated for the remainder of the sampling period (denoted by the “ON”).

organic matter decomposition at the sediments (biological demand) and increased chemical demand from nutrient and metal release. Higher oxygen demand during oxygenation has been observed in several other water bodies, including

Carvins Cove Reservoir and Spring Hollow Reservoir (Gantzer et al., 2009b) and Newman Lake (Moore et al., 1996), and is thought to be able to exceed an induced oxygen demand, or IOD, of 6 (Gantzer et al., 2009b). The increase in IOD of ~3 that

we observed in FCR is within the range of previously observed IODs, also referred to as the induced HOD factor, reported from other oxygenation systems in the literature (1.5–4.0; Beutel, 2003; Gantzer et al., 2009b; Moore et al., 1996). Shallow reservoirs such as FCR are expected to experience induced HOD factors at the high end of this range due to the larger fraction of oxygen demand exerted at the sediments compared to the overlying shallow water column (Beutel, 2003).

Between the two operational periods, we observed a very small increase in the IOD from 2.86 to 3.01, most likely due to the greater biological and chemical oxygen demand in the hypolimnion during the second operational phase compared to the first operational phase. In the second operational phase, the water column was much warmer, thereby accelerating respiration and decomposition processes, and there was much higher chemical demand: reduced Fe, Mn, and P concentrations were much higher in the hypolimnion than in the first operational phase. Despite the increase in HOD due to SSS operation, the observed ability of the SSS system to linearly raise DO concentrations during both operational phases indicates that the SSS system design appears to be adequate in its capacity to overcome the corresponding increases in oxygen demand in FCR, regardless of the starting hypolimnetic oxygen concentrations.

Although SSS operation increased HOD in this short term experiment, it has been hypothesized that HOD will decrease after several years of oxygenation (Gantzer et al., 2009b). Long-term (several year) monitoring programs should be implemented to determine the behavior of HOD after continuous SSS operation.

4.3. SSS suppressed the internal loading of reduced elements

Our data indicate that SSS operation was able to suppress Fe and Mn release from the sediments. After seven days of hypoxia at the sediment–water interface, soluble Fe and Mn release coincided with maximum oxygen depletion prior to SSS reactivation. Upon the reactivation of the SSS on 1 August, the release of Fe and Mn, and potentially P, decreased from the sediments, indicating that the SSS was able to suppress additional internal loading.

During the entire sampling period, almost all of the total Mn in the hypolimnion was in the soluble form, while most of the total Fe was in the particulate form because Fe oxidizes much more rapidly than Mn (Davison, 1993; Balzer, 1982; Bryant et al., 2011). Evidence of the different kinetic rates is shown in Fig. 8 following reactivation of the SSS on 1 August. First, the extreme vertical gradients in the concentrations of both soluble and particulate metals were essentially eliminated before the next sampling event on 7 August, indicating that the hypolimnion was close to completely mixed due to SSS operation. As shown in Fig. 3, the mixing from the SSS also eliminated the oxygen concentration gradient in the hypolimnion, exposing the soluble Fe and Mn initially present in the anoxic bottom of the hypolimnion to higher oxygen concentrations. Simultaneously, oxygen introduced by the SSS raised the mean oxygen concentration in the hypolimnion. As a result, the soluble Fe concentrations decreased slowly,

presumably forming particulate Fe. Indeed, total Fe continued to increase at 8 m depth until 21 August, suggesting an initial accumulation of suspended particulate Fe forming as a result of rapid oxidation in the bottom of the reservoir. After 28 August, total Fe began to decrease in the hypolimnion, suggesting that particulate Fe was removed from the hypolimnion via settling onto the reservoir sediments.

The different behavior of the total and soluble Mn concentrations in the hypolimnion is quite noticeable in Fig. 8. Although the vast majority of the measured Mn was in the soluble form throughout the entire monitoring period, the vertical hypolimnetic gradient in Mn was again eliminated by the initial mixing following SSS reactivation on 1 August. In contrast to Fe, however, the soluble Mn concentration remained relatively constant for the remainder of the sampling period.

Adding oxygen to the hypolimnion of a lake or reservoir does not stop the reduction of Fe and Mn. What it does do, when effectively applied, is to push the oxic–anoxic boundary out of the water column and into the sediments (Gantzer et al., 2009a; Bryant et al., 2011). This means that the oxidation process due to oxygenation can begin within the sediments, effectively reducing the accumulation of soluble Fe and Mn in the water column. The fact that Fe oxidizes much more rapidly than Mn (Davison, 1993; Balzer, 1982; Bryant et al., 2011) means that it is easier to control the accumulation of soluble Fe in the hypolimnion than it is to control the accumulation of soluble Mn. Beginning oxygenation early in the summer prior to the onset of thermal stratification may be an effective strategy to prevent the accumulation of soluble metals in the hypolimnion.

The suppression of Fe and Mn internal loading and accumulation in the water column by hypolimnetic oxygenation was also reported in Carvins Cove Reservoir, a reservoir with a linear bubble-plume diffuser system (Bryant et al., 2011; Gantzer et al., 2009a). However, to the best of our knowledge, there have been no reports of the successful control of Fe and Mn – or P – due to SSS or side stream operation.

It is not clear why there was a 6-week delay in Fe and Mn internal loading during the deactivation period in July, despite prolonged hypoxia at the sediment–water interface. One explanation may be that our deepest nutrient and metal samples were collected 1.3 m above the reservoir sediments, and therefore there was likely nutrient and metal release that we were unable to observe. Another plausible explanation is that there may have been a shift in the sediment microbial community as a result of oxygenation, altering nutrient transformations and sediment release. As observed in Carvins Cove Reservoir, the delayed response in nutrient release may be explained by microbes adapting to altered fluxes in oxygen concentrations (Bryant et al., 2012).

Our data suggest that SSS operation may have altered P release from FCR sediments, but the evidence was not as conclusive as it was for Fe and Mn. Throughout July, during the second deactivation phase, FCR received high external P loads due to large rain events, which potentially may have contributed P to the hypolimnion. However, the strong thermal structure throughout this period, as demonstrated by the metalimnetic oxygen minimum, likely prevented entrainment of P from epilimnion to hypolimnion: consequently, it is

unlikely that these external nutrients entering FCR during the rain events reached the hypolimnion. Furthermore, the much shorter hydraulic residence time of the reservoir during the rain events in mid-July further supports our hypothesis that the external P loads did not contribute to the increased P observed in the hypolimnion. The residence time during these rain events decreased from a mean of 247 days to approximately 10 days, and in turn likely flushed the external loads of P out of the reservoir quickly. The increase in epilimnetic P due to the storm events occurred 14 days before the largest increase in P at the sediments (Fig. 7E); therefore, with a residence time of 10 days and strong thermocline at that time, those epilimnetic and hypolimnetic P dynamics were likely not linked to one another.

5. Conclusion

Our data strongly suggest that SSS is a viable option for improving water quality in FCR, a shallow, eutrophic drinking water reservoir. However, longer-term studies are recommended to evaluate the efficacy of SSS operation. Specifically, multiple years of monitoring will be required to determine if HOD decreases over time, as well as if long-term hypolimnetic oxygenation is able to suppress the internal loading of P. In summary, side stream supersaturation hypolimnetic oxygenation systems may be a favorable management strategy for shallow (<10 m) water bodies.

Acknowledgments

We thank the staff at the Western Virginia Water Authority for their long-term support and funding. In particular, we would like to thank Cheryl Brewer, Jamie Morris, Jeff Booth, Bob Benninger, and Gary Robertson. Kevin Bierlein, Christina Urbanczyk, and Bobbie Niederlehner provided critical help in the field and laboratory. This work was supported by the Virginia Tech Department of Biological Sciences.

Appendix A. Supplementary data

Supplementary data related to this article can be found at <http://dx.doi.org/10.1016/j.watres.2014.09.002>.

REFERENCES

- Ashley, K.I., 1985. Hypolimnetic aeration: practical design and application. *Water Res.* 19 (6), 735–740.
- Ashley, K.I., Hay, S., Scholten, G.H., 1987. Hypolimnetic aeration: field test of the empirical sizing method. *Water Res.* 21, 223–227.
- AWWA, 1987. Research needs for the treatment of iron and manganese. *J. Am. Water Works Assoc.* 79, 119–122.
- Balzer, W., 1982. On the distribution of iron and manganese at the sediment/water interface: thermodynamic versus kinetic control. *Geochim. Cosmochim. Acta* 46, 1153–1161.
- Beutel, M.W., 2003. Hypolimnetic anoxia and sediment oxygen demand in California drinking water reservoirs. *Lake Reserv. Manag.* 19 (3), 208–221.
- Beutel, M.W., 2006. Inhibition of ammonia release from anoxic profundal sediments in lakes using hypolimnetic oxygenation. *Ecol. Eng.* 28 (3), 271–279.
- Beutel, M.W., Horne, A.J., 1999. A review of the effects of hypolimnetic oxygenation on lake and reservoir water quality. *Lake Reserv. Manag.* 15 (4), 285–297.
- Bryant, L.D., Hsu-Kim, H., Gantzer, P.A., Little, J.C., 2011. Solving the problem at the source: controlling Mn release at the sediment–water interface via hypolimnetic oxygenation. *Water Res.* 45 (19), 6381–6392.
- Bryant, L.D., Little, J.C., Burgmann, H., 2012. Response of sediment microbial community structure in a freshwater reservoir to manipulations in oxygen availability. *FEMS Microbiol. Ecol.* 80 (1), 248–263.
- Chow, V.T., 1959. *Open-channel Hydraulics*. McGraw-Hill Book Company, New York, New York.
- CH2M HILL, 2013. Assessment of Technologies for Dissolved Oxygen Improvement in J.C. Boyle Reservoir. CH2M HILL, Portland, Oregon.
- Cooke, G.D., Kennedy, R.H., 2001. Managing drinking water supplies. *Lake Reserv. Manag.* 17 (3), 157–174.
- Cooke, G.D., Welch, E.B., Peterson, S., Nichols, S.A., 2005. *Restoration and Management of Lakes and Reservoirs*, third ed. CRC Press, Boca Raton, Florida.
- Davis, W.S., Fay, L.A., Herdendorf, C.E., 1987. Overview of USEPA/Clear Lake Erie sediment oxygen demand investigations during 1979. *J. Great Lakes Res.* 13 (4), 731–737.
- Davison, W., 1993. Iron and manganese in lakes. *Earth-Sci. Rev.* 34, 119–163.
- Downing, J.A., Prairie, Y.T., Cole, J.J., et al., 2006. The global abundance and size distribution of lakes, ponds, and impoundments. *Limnol. Oceanogr.* 51 (5), 2388–2397.
- Fast, A.W., Lorenzen, M.W., 1976. Synoptic survey of hypolimnetic aeration. *J. Environ. Eng. Div.* 102, 1161–1173.
- Fast, A.W., Overholtz, W.J., Tubb, R.A., 1975. Hypolimnetic oxygenation using liquid oxygen. *Water Resour. Res.* 11 (2), 294–299.
- Fast, A.W., Overholtz, W.J., Tubb, R.A., 1977. Hyperoxygen concentrations in the hypolimnion produced by injection of liquid oxygen. *Water Resour. Res.* 13 (2), 474–476.
- Gantzer, P.A., 2011. Grand Bay, MS SDOX Oxygen Injection Monitoring. Gantzer Water Resources Engineering, LLC, Kirkland, Washington.
- Gantzer, P.A., Bryant, L.D., Little, J.C., 2009a. Controlling soluble iron and manganese in a water-supply reservoir using hypolimnetic oxygenation. *Water Res.* 43 (5), 1285–1294.
- Gantzer, P.A., Bryant, L.D., Little, J.C., 2009b. Effect of hypolimnetic oxygenation on oxygen depletion rates in two water-supply reservoirs. *Water Res.* 43 (6), 1700–1710.
- Grant, M.G., 1991. *Isco Open Channel Flow Measurement Handbook*, third ed. Isco, Inc., Lincoln, Nebraska.
- Idso, S.B., 1973. On the concept of lake stability. *Limnol. Oceanogr.* 18 (4), 681–683.
- Liborius, L., Søndergaard, M., Jeppesen, E., et al., 2009. Effects of hypolimnetic oxygenation on water quality: results from five Danish lakes. *Hydrobiologia* 625 (1), 157–172.
- Lorenzen, M.W., Fast, A.W., 1977. *A Guide to Aeration/Circulation Techniques for Lake Management*. Report EPA-600/3-77-004. U.S. EPA, Corvallis, Oregon.
- Matthews, D.A., Effler, S.W., 2006. Assessment of long-term trends in the oxygen resources of a recovering urban lake, Onondaga Lake, New York. *Lake Reserv. Manag.* 22 (1), 19–32.
- McGinnis, D.F., Little, J.C., 2002. Predicting diffused-bubble oxygen transfer rate using the discrete-bubble model. *Water Res.* 36, 4627–4635.

- MEA, 2005. *Ecosystems and Human Well-being: Synthesis*. Island Press, Washington, DC.
- Moore, B.C., Chen, P.H., Funk, W.H., Yonge, D., 1996. A model for predicting lake sediment oxygen demand following hypolimnetic aeration. *Water Resour. Bull.* 32, 723–731.
- Mortimer, C.H., 1941. The exchange of dissolved substances between mud and water in lakes. *J. Ecol.* 29, 280–329.
- Noll, M.R., 2011. Phosphorus cycling in a managed lake ecosystem: seasonal and longer-term trends. *Appl. Geochem.* 26, S234–S237.
- OWRB, 2012. *Lake Thunderbird Water Quality 2011*. Oklahoma Water Resources Board, Oklahoma City, Oklahoma.
- OWRB, 2013. *Lake Thunderbird Water Quality 2012*. Oklahoma Water Resources Board, Oklahoma City, Oklahoma.
- Read, J.S., Hamilton, D.P., Jones, I.D., Muraoka, K., et al., 2011. Derivation of lake mixing and stratification indices from high-resolution lake buoy data. *Environ. Model. Softw.* 26 (11), 1325–1336.
- Scheffer, M., 2004. *Ecology of Shallow Lakes*. Kluwer Academic Publishers, Dordrecht, Netherlands.
- Schindler, D.W., 1977. Evolution of phosphorus limitation in lakes. *Science* 195 (4275), 260–262.
- Schindler, D.W., Hecky, R.E., Findlay, D.L., et al., 2008. Eutrophication of lakes cannot be controlled by reducing nitrogen input: results of a 37-year whole-ecosystem experiment. *Proc. Natl. Acad. Sci. U.S.A.* 105 (32), 11254–11258.
- Sherman, B., Bryant, L.D., Mobley, M.H., Ford, P., McGinnis, D.F., Singleton, V.L., Schafran, G., Little, J.C., 2012. Review of Oxygenation Technologies with Special Reference to Application in the Canning River. CSIRO. Report to W. Australia Dept. of Water.
- Singleton, V.L., Little, J.C., 2006. Designing hypolimnetic aeration and oxygenation systems – a review. *Environ. Sci. Technol.* 40 (24), 7512–7520.
- Smith, V.H., 1982. The nitrogen and phosphorous dependence of algal biomass in lakes – an empirical and theoretical analysis. *Limnol. Oceanogr.* 27 (6), 1101–1112.
- Toffolon, M., Ragazzi, M., Righetti, M., Teodoru, C.R., et al., 2013. Effects of artificial hypolimnetic oxygenation in a shallow lake. Part 1: phenomenological description and management. *J. Environ. Manage.* 114, 520–529.
- Wetzel, R.G., 2001. *Limnology: Lake and River Ecosystems*, third ed. Academic Press, San Diego, California.
- Wu, R.S.S., Zhou, B.S., Randall, D.J., Woo, N.Y.S., Lam, P.K.S., 2003. Aquatic hypoxia is an endocrine disruptor and impairs fish reproduction. *Environ. Sci. Technol.* 37 (6), 1137–1141.
- Wyman, B., Stevenson, L.H., 1991. *Dictionary of Environmental Science*. Facts On File, Inc., New York, New York.
- Yajima, H., Imberger, J., Dallimore, C., 2009. Evaluation of the intrusion generated by a submerged contact chamber of hypolimnetic oxygenator in a reservoir. *Int. J. River Basin Manage.* 7 (4), 415–422.
- Zaccara, S., Canziani, A., Roella, V., Crosa, G., 2007. A northern Italian shallow lake as a case study for eutrophication control. *Limnology* 8 (2), 155–160.
- Zaw, M., Chiswell, B., 1999. Iron and manganese dynamics in lake water. *Water Res.* 33 (8), 1900–1910.